

See discussions, stats, and author profiles for this publication at: <https://www.researchgate.net/publication/268450624>

Unusual Dewetting of Thin Polymer Films in Liquid Media Containing a Poor Solvent and a Nonsolvent

ARTICLE in LANGMUIR · NOVEMBER 2014

Impact Factor: 4.46 · DOI: 10.1021/la503319w · Source: PubMed

READS

62

5 AUTHORS, INCLUDING:



[Lin Xu](#)

University of Minho

15 PUBLICATIONS 136 CITATIONS

[SEE PROFILE](#)



[Ashutosh Sharma IITK](#)

Indian Institute of Technology Kanpur

335 PUBLICATIONS 7,410 CITATIONS

[SEE PROFILE](#)



[Tongfei Shi](#)

Chinese Academy of Sciences

91 PUBLICATIONS 667 CITATIONS

[SEE PROFILE](#)

Unusual Dewetting of Thin Polymer Films in Liquid Media Containing a Poor Solvent and a Nonsolvent

Lin Xu,[†] Ashutosh Sharma,^{*,‡} Sang Woo Joo,[†] Hui Liu,^{§,||} and Tongfei Shi^{*,§}

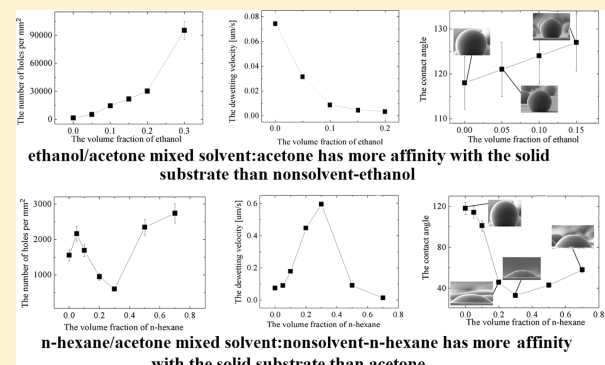
[†]School of Mechanical Engineering, Yeungnam University, Gyeongsan 712-749, South Korea

[‡]Department of Chemical Engineering, Indian Institute of Technology, Kanpur 208016, India

[§]State Key Laboratory of Polymer Physics and Chemistry, Changchun Institute of Applied Chemistry, Chinese Academy of Sciences, Changchun 130022, P. R. China

^{||}Department of Physics, Jilin University, Changchun 130012, P. R. China

ABSTRACT: We investigate the control of pattern size and kinetics in spontaneous dewetting of thin polymer films (polystyrene) that are stable to thermal annealing by annealing in a poor solvent (acetone)/nonsolvent (ethanol or *n*-hexane) liquid mixture. Dewetting occurs by the formation and growth of circular holes that coalesce to form droplets. The influence of the nature and the volume fraction of the nonsolvents on the contact angle of polymer droplets, number density of holes, and the kinetics of holes formation and growth is studied. Addition of ethanol greatly increases the hole density and slows down the kinetics substantially, while affecting only a small change in wettability. *n*-Hexane addition shows an interesting nonmonotonic response in decreasing the hole density and contact angle in the volume fraction range of 0–0.3 but an opposite effect beyond that. Although the two nonsolvents chosen cannot by themselves induce dewetting, their relative affinity for the solid substrate vis-à-vis acetone can strongly influence the observed dewetting scenarios that are not understood by the existing theoretical considerations. *n*-Hexane, for example, has great affinity for silicon substrate. In addition to the changes in wettability, viscosity, and film interfacial tension engendered by the nonsolvents, the possibility of the formation of adsorbed liquid layers at the substrate–polymer interface, which can modify the interfacial friction and slippage, needs to be considered.



INTRODUCTION

Spontaneous instability and dewetting of ultrathin (<100 nm) liquid polymer films on solid substrates have attracted intense attention because of the widespread applications of the films in physics, materials, polymer science, chemistry, and engineering of highly confined matter.^{1–46} Dewetting of thin polymer films not only relates to many fundamental phenomena in confined systems, such as spinodal and nucleative processes wetting and adhesion, but it is also an attractive self-organization-based technique for micro/nanopatterning of soft matter.^{4–8} An ultrathin liquid film is often unstable owing to attractive interactions (e.g., van der Waals) between the two proximal interfaces and dewets by the formation of growing and coalescing holes. Much of the previous work relates to thermally triggered dewetting, where the film is heated beyond its glass transition temperature.^{9–20} Here we focus on two outstanding questions in thin film dewetting: (1) how to destabilize the polymer films that are otherwise stable (e.g., by thermal annealing) on a high-energy substrate that encourages spreading rather than rupture and retraction and (2) how to control the length scale or the density of features in the dewetted structures. Both of these questions are of paramount relevance in the self-organized patterning by dewetting.

Dewetting of thin films is a good model system for investigating the low dimensional physics of polymer chains in a melt, but most of dewetting studies have been by thermal annealing above the glass transition. Gabriele and co-workers^{21,22} showed the transition from the elasticity-dominated regime to a viscosity-dominated regime via the dewetting kinetics of holes growth and the shape of the rim. Recently, Tsui's research group^{23–25} reported the change of the glass transition temperature of polymer chains with the film thickness by a thermal dewetting process. Another route to trigger thin film dewetting is by exposure to the vapors of a good solvent, which reduces the glass transition temperature below room temperature.^{26–30} The solvent-vapor-induced dewetting largely parallels the characteristics of the thermal dewetting in that the stabilizing surface tension is largely unaltered and thus the length scale of the surface instability cannot be varied except by a change in the film thickness and by relaxation of residual stresses in the high molecular weight films.^{26,27} Thus, control and miniaturization of the instability

Received: August 21, 2014

Revised: November 16, 2014

Published: November 17, 2014



length scale remains a major challenge during a thermal dewetting process and solvent-vapor-induced dewetting because of the relative high surface tension between polymer and air or solvent vapor. Further, the instability and dewetting of the polymer films (such as polystyrene) that lack significant non-van der Waals or polar interactions with the substrate are determined by the net van der Waals interactions. Such films are stable on high-energy substrates (such as oxide stripped silicon wafer), where the adhesive van der Waals interaction between the substrate and the film exceeds the cohesive interactions in the film.^{6,39,46} Thus, an important question is how to engender instability and dewetting in a film that is stable in air. In this context, the role of annealing under liquids (mixtures of solvents, poor solvents, and nonsolvents) that may induce destabilizing forces other than the van der Waals^{6,39} ones becomes important.^{31–35}

A recent attractive room temperature technique for the control of instability and dewetting by reduction of interfacial tension is recently proposed where a polymer thin film is annealed under a homogeneous liquid mixture of a good solvent (methyl ethyl ketone, MEK) and a nonsolvent (water), to which a poor solvent (acetone) may be added to facilitate the formation of a single phase liquid.^{31,32} These works^{31–33} have shown that the characteristic length scale of the surface instability leading to dewetting and the dewetted structures can be reduced by about two orders of magnitude in a liquid solvent mixture compared to the dewetting induced by thermal and the solvent vapor annealings. This is because the presence of a liquid solvent can greatly decrease the interfacial tension, and at the same time, the presence of a nonsolvent at a suitable concentration prevents dissolution of the polymer. Further, the destabilizing van der Waals interactions may also be significantly altered by introducing a stronger electrostatic attractive force in the media containing water.^{31,32} This technique^{31,32} successfully utilized the dewetting of thin polymer films in a solvent–nonsolvent liquid mixture (MEK/water) to engineer 40 nm to micron-sized polymeric domains and nanolens arrays. This brings down the size of physical self-organization-based patterning to the domain of chemical self-assembly. Although water is a nonsolvent, it has been argued that the polymer chains exposed to deaerated water over long periods can acquire sufficient mobility to form a nanopattern.^{34,35}

Our recent work³³ explored dewetting of stable polystyrene (PS) films on oxide stripped silicon wafers in liquid acetone, which is a poor solvent for PS and thus prevents its dissolution while allowing sufficient polymer mobility for dewetting. These films were resistant to dewetting by thermal annealing in air. It was found that the polar interactions^{6,39} engendered by acetone are largely responsible for the instability and dewetting in this system aided by the possibility of nanophase separation near the substrate owing to a strong affinity of acetone for oxide-stripped silicon.³³ During the dewetting in a liquid solvent, the solvent molecules can enter in the film in sufficient amounts to decrease the glass transition temperature below room temperature and, at the same time, decrease the interfacial tension. Thus, the dewetting structures, mechanisms, and kinetics in liquid solvents and their mixtures are more complex and far richer than in the thermal and vapor-phase annealing, thus offering greater flexibility in the control of dewetting kinetics and patterns. However, the investigation of confined polymers in liquid mixtures of solvents/poor solvents/nonsolvents is still in its infancy and a deeper understanding is required to address

many open questions on the role of nonsolvent beyond prevention of polymer dissolution. In addition, the dewetting of thin polymer film in liquid solvents is also a good model to study fundamentals of surface-induced nanophase separations and low-dimension soft matter physics of polymer chains in solvents.

In this paper, we investigate instability and dewetting of thin PS films on silicon wafers annealed under two different liquid mixtures of a poor solvent (acetone) and a nonsolvent (acetone/ethanol and acetone/*n*-hexane). Both *n*-hexane and ethanol are nonsolvents for PS and both are miscible with acetone under a wide range of mixture compositions studied here.^{47,48} In the first mixture, acetone (poor solvent) has greater affinity for the substrate than the nonsolvent (ethanol), whereas in the second mixture, the nonsolvent (*n*-hexane) has more affinity for the substrate than the poor solvent (acetone). Among the nonsolvents, *n*-hexane also has greater affinity for the substrate than ethanol. We study the effects of the nature of the nonsolvent and the mixture composition on the length and time scales of dewetting to gain an understanding of the roles of nonsolvent in controlling the behavior of thin polymer films. Indeed, we show that the addition of a nonsolvent can strongly influence the dewetting behavior of thin polymer films annealed under a poor solvent/nonsolvent mix, thus allowing an unprecedented control over the equilibrium and dynamics of thin film pattern formation, even in the films that are stable in air by thermal annealing.

EXPERIMENTAL SECTION

Thin, spin-coated films of PS were annealed in the preprepared homogeneous liquid mixtures of acetone/*n*-hexane and acetone/ethanol at room temperature. The solvent volume used was 40 mL, in which a PS film of ~1 cm² area was kept completely immersed. Polystyrene ($M_w = 390$ kg/mol, $M_w/M_n = 1.1$, from Sigma-Aldrich) was dissolved in toluene and spin-coated on the Si wafers without the oxide layer. Prior to spin-coating, the wafers were cleaned with deionized water and acetone, boiled in a 2/1 (v/v) solution of 98% H₂SO₄/30% H₂O₂ for 30 min, thoroughly rinsed with deionized water, and dried with compressed nitrogen. The native oxide layer was removed by hydrofluoric acid. The thickness of all films was measured by ellipsometry. In the experiments, the thickness of the PS films was kept constant at 67 ± 2 nm to directly assess the effects of liquid composition. The residual solvent was completely removed by placing the films in a vacuum oven for 48 h at room temperature. However, the droplets freeze immediately after their removal from the liquid owing to a rapid increase in viscosity. The change of the PS film morphology was observed with an optical microscope (OM) in reflection mode with a CCD camera attachment. The equilibrium contact angles of PS droplets on the solid substrate were examined by placing the substrate vertically in the field emission scanning electron microscope (FESEM) to see the side view of these droplets. The equilibrium contact angles of solvents on the solid substrate were measured by drop shape analysis at room temperature.

RESULTS AND DISCUSSION

Thin PS films were annealed in liquids as shown in the schematic Figure 1. It was found that the PS films dewet in acetone (poor solvent) but remain stable in *n*-hexane and ethanol (nonsolvents), as expected.

The interaction parameter between a polymer and a solvent is a guide to determine the solvent quality for the polymer chain. A smaller interaction parameter indicates better solvent quality for the polymer chain. The interaction parameter is related to the square of the difference in solubility parameters³⁶

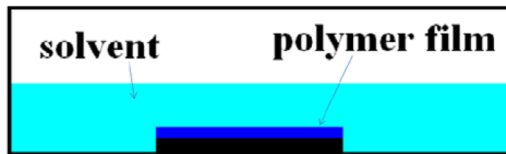


Figure 1. Schematic diagram of the experimental setups.

$$\chi \sim (\delta_A - \delta_B)^2 \quad (1)$$

where χ is the interaction parameter, and δ_A and δ_B are solubility parameters.

Here, δ_{PS} is $18.7 \text{ MPa}^{1/2}$, δ_{acetone} is $19.7 \text{ MPa}^{1/2}$, $\delta_{n\text{-hexane}}$ is $14.9 \text{ MPa}^{1/2}$, and δ_{ethanol} is $26.2 \text{ MPa}^{1/2}$.

According to eq 1, *n*-hexane and ethanol are poorer solvents for PS chains than acetone, but they interact well with acetone to form a solution. Due to their high interaction parameters with PS and acetone, *n*-hexane and ethanol make the PS chains shrink, which should decrease the mobility of the PS chains, as well as somewhat decrease the concentration of acetone in the PS film by a partitioning of acetone in the solution and the polymer. Solvent quality decreases as the temperature is lowered. *n*-Hexane and ethanol cannot drive the motion of PS chains on the solid substrate at room temperature. It was indeed confirmed that the PS films are stable in *n*-hexane and ethanol at room temperature. However, during the dewetting process in the mixture containing acetone, acetone molecules can enter in the PS matrix in copious amounts because the interaction parameter between PS and acetone is lower. Due to the presence of acetone molecules in PS matrix, the glass transition temperature of the PS is lowered below room temperature, thus allowing chain mobility and dewetting. The dewetting process of thin PS film in pure acetone has been studied in our previous work³³ with the finding that the polar interactions induced by the poor solvent engender the instability in this case. This is different from dewetting by thermal and vapor annealings. The high molecular PS films on oxide-stripped silicon wafers were in fact stable. Although vapor acetone annealing did dewet the low molecular weight films, the instability was much stronger in liquid acetone compared to vapor acetone (much higher holes density in liquid acetone).³³

In the following, we investigate the dewetting process of thin polymer film in mixed liquid solvents and the influence of the nature of the nonsolvents on the dewetting process. In our experiment, we added a polar solvent, ethanol, or a nonpolar solvent, *n*-hexane, into acetone, respectively. Further, as will be discussed later, *n*-hexane has more affinity for silicon substrate than acetone and ethanol.

Figure 2 shows the morphologies of PS films during the dewetting process in mixed solvents with different volume fraction of ethanol.

Figure 3 shows the variation of the maximum number density of holes (per mm^2) with the volume fraction of ethanol.

As shown in Figure 3, the number of holes always increases with the increase in the volume fraction of ethanol. When the PS film was treated with the mixed solvent containing more than 40% volume fraction of ethanol, the film became stable.

The kinetics of holes growth is shown in Figure 4. The data in Figure 4 are representative dewetting kinetics of a single hole. The same data from different holes showed less than 10% variation.

Figure 4a shows that the radius of the hole grows linearly with time. Figure 4b shows the plot of the dewetting velocity

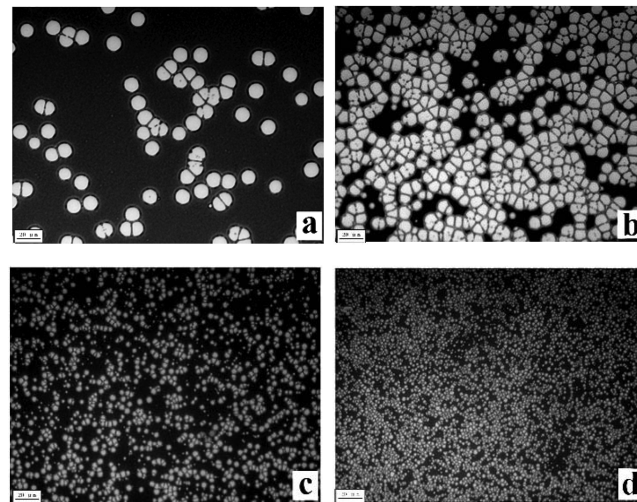


Figure 2. OM images show the morphologies of PS films after the dewetting in mixed solvents with different volume fractions of ethanol at different annealing times: (a) 0%, 3 min; (b) 5%, 5 min; (c) 10%, 8 min; and (d) 30%, 180 min. The size of the bar is $20 \mu\text{m}$.

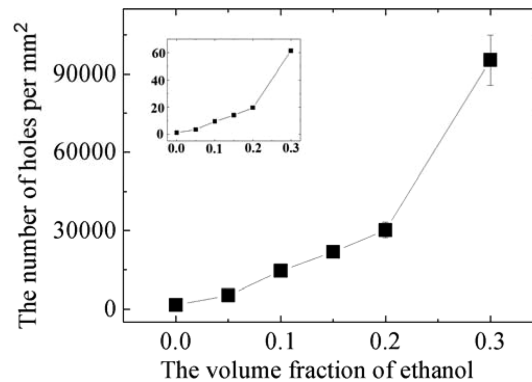


Figure 3. Plot of the number of holes per mm^2 and the volume fraction of ethanol. The inset shows the plot of the ratio of hole density for dewetting in different mixed solvents and dewetting in pure acetone.

and the volume fraction of ethanol. As shown in Figure 4b, the velocity of the hole growth decreases monotonically with the increase in the volume fraction of ethanol. One of the obvious reasons for this observation is that the added nonsolvent (ethanol) can decrease the mobility of PS chains and consequently slow down the dewetting velocity. However, as will be discussed later, factors other than the polymer viscosity also play important roles in determining the kinetics of dewetting.

Next, we consider the dewetting behavior of the thin PS film in the mixture of acetone and *n*-hexane. The results show that the dewetting process is different from that in the mixture of acetone and ethanol. Figure 5 show the morphologies of PS films during the dewetting process in mixed solvents with different volume fractions of *n*-hexane.

Figure 6 shows the plot of the maximum number density of holes and the volume fraction of *n*-hexane. When a small amount of *n*-hexane (5% volume fraction) is added in acetone, the number of holes formed rapidly increases in the mixed solvents compared to the pure acetone. With a further increase of the volume fraction of *n*-hexane, it is found that the hole density does not change monotonously but first decreases and

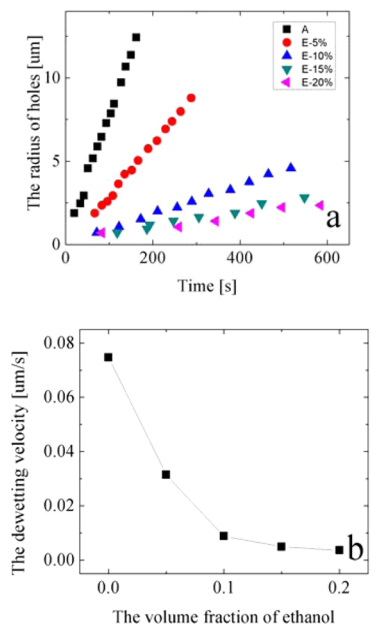


Figure 4. (a) Kinetics of holes growth and (b) plot of the dewetting velocity and the volume fraction of ethanol.

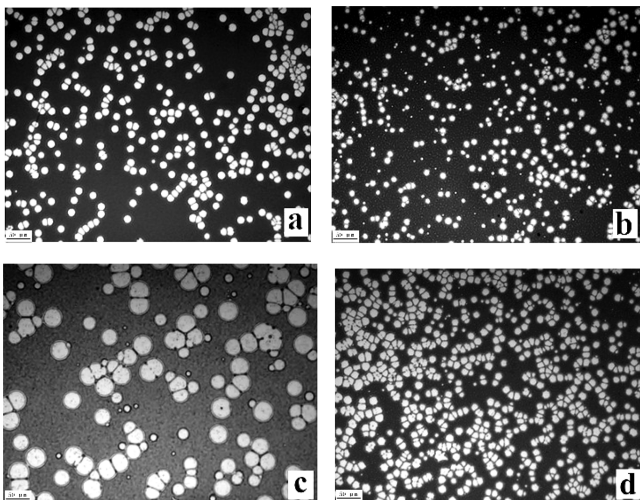


Figure 5. OM images show the morphologies of PS films after the dewetting in mixed solvents with different volume fractions of *n*-hexane at different annealing times: (a) 0%, 3 min; (b) 5%, 2 min; (c) 30%, 0.5 min; (d) 70%, 8 min. The size of the bar is 50 μm .

then increases again. When the PS film was placed in the mixed solvent containing 90% volume fraction of *n*-hexane, the PS film became stable because of insufficient lowering of the glass-transition temperature.

Figure 7 shows the kinetics of holes growth. As shown in Figure 7a, the dewetting velocity is nearly constant in the time range studied until the holes start to coalesce. Figure 7b shows an interesting nonmonotonic variation of the dewetting velocity with the volume fraction of *n*-hexane. The velocity of contact line first increases with an increase in the volume fraction of *n*-hexane, but it decreases beyond a volume fraction of ~ 0.3 . Addition of a nonsolvent such as *n*-hexane is expected to decrease the mobility of PS chains and is thus expected to always decrease the kinetics of dewetting. However, Figure 7b shows that the velocity of hole growth first increases with the increase in the volume fraction of *n*-hexane. Clearly, factors

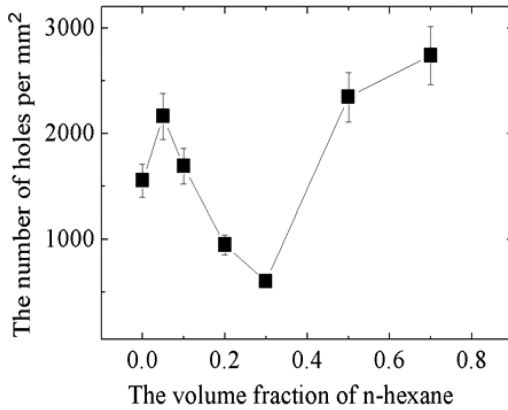


Figure 6. Plot of the mean number of holes per square millimeter versus the volume fraction of *n*-hexane.

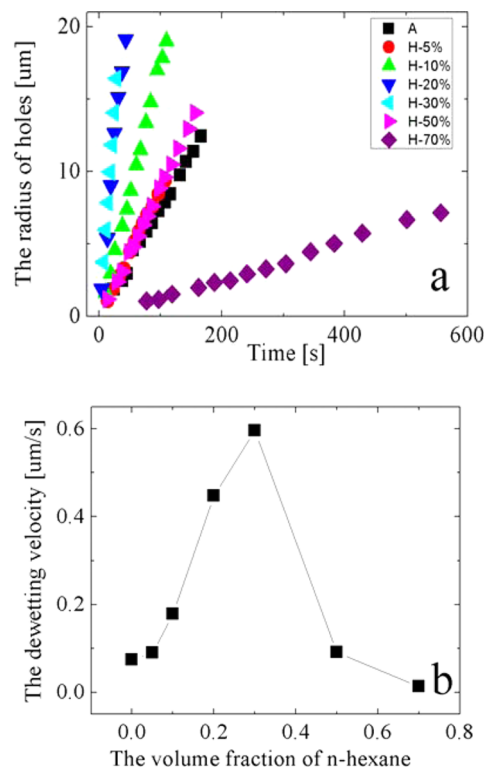


Figure 7. (a) Kinetics of holes growth and (b) plot of the dewetting velocity versus the volume fraction of *n*-hexane.

beyond the transport parameters, such as the chain mobility and viscosity, also need to be considered.

Spontaneous dewetting of thin liquid films have three major stages:^{19,20,37–40} (1) formation of holes by increasing deformations of the film surface engendered by a surface instability, (2) growth of holes by retraction of their contact lines, and finally, (3) coalescence of holes, resulting in droplets. We now examine the kinetics of the first two stages in the greater details.

Figure 8 depicts the kinetics of the formation of holes by plotting the number density of holes with time. The first striking feature is an almost constant density of holes in pure acetone after their initial rapid formation, indicating that all the holes form nearly simultaneously within a narrow window of time. However, in the cases of the two mixed solvents, the number of holes increases gradually over longer times, showing

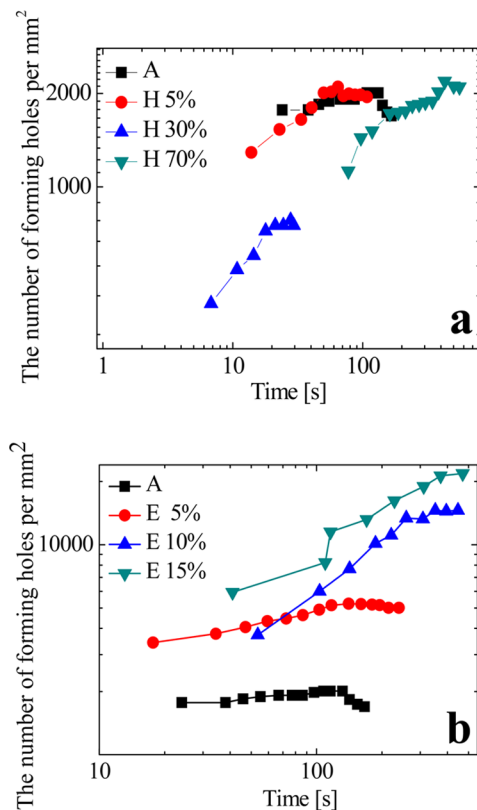


Figure 8. Plot of the number of forming holes per square millimeter versus time: (a) for the series of mixed solvents between acetone and *n*-hexane and (b) for the series of mixed solvents between acetone and ethanol.

the formation of newer holes even as the holes formed earlier are in their phase of expansion.

Continued formation of holes over a wide window of time is also reflected in the wider size distribution of holes, as seen in the Figures 2 and 5, where dewetting in the mixed solvents produces inhomogeneities of hole diameters. With an increased volume fraction of ethanol, the kinetics of hole formation becomes sluggish (Figure 8b), which is also correlates with the slowing of contact-line retraction (Figure 4). Similarly, there is also a clear correlation between the kinetics of hole formation (Figure 8a) and hole growth (Figure 7) as the volume fraction of *n*-hexane is increased. The most rapid formation and growth of holes both occur at a volume fraction of 0.3. It is a possibility that the rapid growth of the holes that form first could inhibit the formation of other potential holes and lead to the decrease of hole density, as in the case of an *n*-hexane fraction of 0.3.

To understand the results related to the effects of nonsolvents on the number density of holes and the kinetics of hole formation and growth, we also quantified the equilibrium contact angles of the dewetted PS droplets (Figure 9a,b) and the contact angles of the solvents on the oxide-stripped silicon wafers (Figure 9c).

From Figure 9c, the wetting ability of various solvents for the silicon substrate follows the order *n*-hexane > acetone > ethanol. *n*-Hexane completely spread on the substrate. Another indicator of the affinity of a liquid for a substrate in air is the energy of adhesion, $\Delta G_{IL} = \gamma_{IL} - \gamma_1 - \gamma_L$, which together with the Young's equation $\gamma_L \cos \theta + \gamma_{IL} = \gamma_1$ gives $\Delta G_{IL} = -\gamma_L(1 + \cos \theta)$. Here γ_{ij} are interfacial tensions and the subscripts correspond to silicon substrate (1) and solvent (L); $\theta > 0$ is the

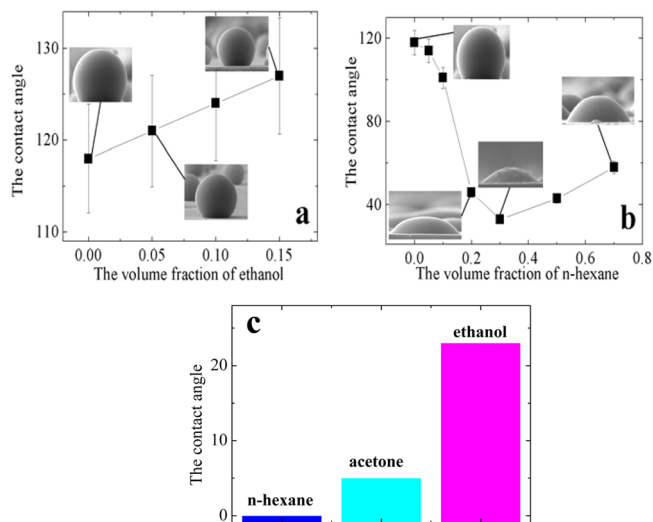


Figure 9. Equilibrium contact angles of PS droplets on the solid substrate are shown: (a) the mixed solvents with different volume fractions of ethanol, (b) the mixed solvents with different volume fractions of *n*-hexane (the insets in parts a and b are the SEM images of the side view of PS droplets), and (c) the equilibrium contact angles of the three different solvents on the solid substrate. The error bar of the contact angles is less than 5%.

equilibrium contact angle. More negative ΔG indicates greater reduction in interfacial energy on adhesion. Thus, the affinity of acetone for the Si substrate is stronger than that of ethanol (ΔG values for acetone is -46.5 mN/m and for ethanol is -43.3 mN/m). However, in the case of hexane with complete spreading, the Young's equation cannot be used. However, it should be noted that the above discussion pertains to affinities in air, but the important issue in our context is the affinities in the three-phase system Si–polymer–liquid.

The dewetted droplets of PS were examined by placing the substrate vertically in the FESEM to measure the contact angle of PS droplets after completion of dewetting.

The contact angle of PS droplets on the substrate in the presence of acetone/nonsolvent mixture can be interpreted with the help of Young's equation:

$$\gamma_{23} \cos \theta + \gamma_{12} = \gamma_{13} \quad (2)$$

where γ_{ij} are interfacial tensions and the subscripts correspond to silicon substrate (1), polymer (2), and liquid mixture (3); θ is the contact angle.

According to the Young's equation: $\cos \theta_{\text{polymer on Si}} = (\gamma_{\text{solvent/Si}} - \gamma_{\text{polymer/Si}})/\gamma_{\text{polymer/solvent}}$. As $\theta_{\text{polymer on Si}} > 90^\circ$, $\cos \theta_{\text{polymer on Si}}$ is smaller than zero in the case of the mixed solvent between acetone and ethanol. When the nonsolvent (ethanol) fraction increases, both $\gamma_{\text{polymer/solvent}}$ and $\gamma_{\text{solvent/Si}}$ should increase somewhat. However, both of these changes should decrease the contact angle, $\theta_{\text{polymer on Si}}$, which is the opposite of our experimental results. Clearly, the situation is more complex as $\gamma_{\text{polymer/Si}}$ is not simply the interfacial tension of dry polymer but that in its saturated state with the solvents. Thus, $\gamma_{\text{polymer/Si}}$ should also increase by the addition of a nonsolvent (ethanol). This is aided by the shrinkage of polymer chains to form globules with enhanced interchain interaction³⁶ but weakened interaction with the substrate. Further, with increased ethanol fraction, the Si–PS interface may also contain more of ethanol, thus increasing the interfacial energy of this composite interface. However, in comparison with the case of *n*-hexane

discussed below, which has good affinity for the Si interface, ethanol accumulation at this interface should be minimal and the small changes in the contact angle seem to be of entropic origin.

The case of *n*-hexane addition is rather more curious (Figure 9b) in that the contact angle decreases sharply from around 120° in pure acetone to around 30° at an *n*-hexane volume fraction of 0.3 and then recovers slowly to around 60° at an *n*-hexane volume fraction of 0.7. In the first stage or regime of low *n*-hexane fraction, PS-mixed solvents interfacial tension (and thus contact angle) should increase with the addition of a nonsolvent. Thus, this finding indicates a concurrent reduction in the PS-substrate (silicon wafer) interfacial tension and a possible increase in the substrate-solvent interfacial tension that dominates over the increase in the PS-mixed solvents interfacial tension below a moderate volume fraction of *n*-hexane (0–0.3). The contact angles of pure acetone and pure *n*-hexane on PS film were measured to be 12° and 10° (error 1°), respectively. According to the Young's equation

$$\gamma_{\text{polymer/solvent}} = \gamma_{\text{polymer/air}} - \gamma_{\text{solvent/air}} \cos \theta_{\text{solvent on polymer film}}$$

Thus, $\gamma_{\text{polymer/solvent}}$ should increase by a few mN/m with the increase of the volume fraction of *n*-hexane to 0.3 because the surface tension of *n*-hexane is smaller than that of acetone by about 5 mN/m and the contact angle $\theta_{\text{solvent on polymer film}}$ is rather invariant with the adding of *n*-hexane. The use of eq 2 for a drop of acetone/*n*-hexane mixture on polystyrene would thus show that only a small monotonic increase of γ_{23} cannot explain the great change of the equilibrium contact angles of the dewetted PS droplets from 117° to around 30°, when only 30% volume fraction *n*-hexane is added into mixture with a change in the value of $\cos \theta$ from negative to positive. Clearly, the mixture composition is affecting the PS-substrate (γ_{12}) and substrate-mixture (γ_{13}) interfacial tensions rather more profoundly, which can explain the variation of the contact angle as announced. According to eq 2, $(\gamma_{13} - \gamma_{12})$ must change from negative to positive in the first stage. The first possible reason is that γ_{13} ($\gamma_{\text{solvent/Si}}$) rapidly increases with the adding of *n*-hexane. According to Young's equation, $\gamma_{\text{solvent/Si}} = \gamma_{\text{Si/air}} - \gamma_{\text{solvent/air}} \cos \theta_{\text{solvent on Si}}$, γ_{13} ($\gamma_{\text{solvent/Si}}$) indeed increases with the adding of *n*-hexane because the surface tension of *n*-hexane is smaller. However, this is not sufficient to explain the contact angle variation from 117° to around 30°, when only 30% volume fraction *n*-hexane is added into mixture. The second possible reason is that the Si-polymer interfacial tension (γ_{12}) greatly decreases with the adding of *n*-hexane. Enrichment/adsorption of *n*-hexane at the substrate-polymer interface owing to its strong affinity for the substrate (Figure 9c) could sharply decrease γ_{12} , thus decreasing the contact angle, as observed. In addition, this view also successfully explains the kinetics of holes growth with a sharp decrease in the interfacial friction as discussed later. Thus, some increase of $\gamma_{\text{solvent/Si}}$ and, more importantly, the sharp decrease of $\gamma_{\text{polymer/Si}}$ are the factors that explain a sharp decline in the contact angle in the range of small *n*-hexane fraction. At larger fraction (>0.3), a small increase in the contact angle is similar to the increase seen in the case of ethanol and can be explained by small increases in the polymer-solvent and polymer-substrate interfacial tensions by the entropic effects of the nonsolvent on the polymer chains. Thus, the affinity of the nonsolvent for the substrate can strongly influence the contact angles of the dewetted PS droplets. As the *n*-hexane volume fraction becomes larger (>0.3), the substrate adsorption induced effects should saturate

and a continued slow increase in the PS-mixed solvents interfacial tension together with a decrease in substrate-mixture interfacial tension can once again increase the contact angle somewhat. Clearly, understanding of the contact angle decrease by *n*-hexane addition requires a modification of the PS-substrate interface in a profound way.

The contact angle discussed above reflects the wetting propensity of dewetted PS drops on silicon wafer in the presence of surrounding liquid mix as the droplets freeze in that position upon removal from the liquid. When these droplets were heated in air, their contact angle decreased slowly with time (for example, the droplets of initial contact angle of about 120° obtained by acetone annealing respread to ~30° angle after 12 h of annealing at 180 °C). This is again expected on oxide-denuded silicon, on which the PS film is stable under thermal annealing. This observation clearly indicates the role of acetone and other liquids in producing a large three-phase contact angle leading to dewetting. However, the kinetics of spreading was slow, which is likely due to the modification of reactive silicon surface by adsorption of PS chains (autophobicity)¹³ and growth of even a monolayer of oxide. Both of these factors can change the short-range interactions at the contact profoundly and could produce nonzero, but small, equilibrium contact angles.^{13,39,46}

In what follows, we examine the number density of holes and the kinetics of dewetting in view of the discussion above. As a cautionary note before proceeding further, we note that the experimental results presented, as novel and interesting as they are, are in conflict with our existing theoretical understanding on several counts that we discuss candidly below with an effort to suggest new insights and to stimulate further work on the complex physics of four component (substrate-film-solvent-nonsolvent) unstable thin polymer films.

We first note that the maximum number density of holes, N , in a thin film is governed by a competition between the destabilizing intersurface interactions and stabilizing interfacial tensions (thermodynamic factors) rather than the kinetic or transport factors (viscosity).^{6,14,19,38,39,46}

$$N = \lambda^{-2} \sim [-(\partial^2 \Delta G / \partial h^2) / \gamma_{23}] \quad (3)$$

where λ is the dominant length scale of the instability or the mean distance between the holes, ΔG is the excess energy of the intersurface interactions per unit area, γ_{23} is the PS-solution interfacial tension, and h is the film thickness. A negative value of the spinodal parameter $[-(\partial^2 \Delta G / \partial h^2)]$ indicates spontaneous dewetting by amplification of surface instability. We had earlier shown that owing to closely matched van der Waals properties of PS and organic solutions, the net apolar van der Waals force in such systems is negligible or even slightly stabilizing.³³ The genesis of thin film stability is thus traced to the polar interactions induced by the presence of acetone.^{6,33} It has been shown that the excess thin film energy (and spinodal parameter) can be related to the macroscopic parameters of wetting, $-(\partial^2 \Delta G / \partial h^2) \sim \gamma_{23} f(\theta)$,^{6,39} where $f(\theta)$ is an increasing function of θ , so that N increases with the contact angle, θ . While quantitative evaluations are not possible because there is no direct method to quantify the apolar and polar interactions in this complex multiphase system with likely interfacial segregation of some components, the qualitative picture is fairly clear. The fact that a stronger instability or greater density of holes should result on a more nonwettable substrate (higher θ) is physically understandable, and indeed,

there should be no dewetting or holes when the substrate is completely wettable. The density of holes in Figures 3 (for ethanol) and 6 (for *n*-hexane) indeed generally mirror the variation of contact angles for the respective nonsolvents, as shown in Figure 9a,b. However, in the case of ethanol, this explanation of the change in hole density by a factor of 60 (inset of Figure 3) despite a relatively small change in wettability (117° – 127° in Figure 9a) does not seem to be completely satisfactory and hints at involvement of other factors, such as nanophase separation and slippage at the substrate–polymer interface. As ethanol has much less affinity compared to acetone for silicon substrate, it cannot form an enriched layer displacing acetone, but it could possibly reduce the enrichment of acetone there because of its solubility with ethanol. This factor may reduce the slippage of polymer chains induced by acetone enrichment with increased ethanol fraction. It is known that a decrease in the slippage (characterized by a slip length) increases the hole density.^{39,40} In contrast, addition of *n*-hexane should further increase slip owing to its greater affinity for the substrate and thus reduce the hole density, in addition to the effect on contact angle, as is evident until a volume fraction of 0.3. Beyond that, a saturation of the interface (slippage) should now make the hole density depend only on the contact angle.

Understanding of the kinetics of hole formation and growth is even more complex compared to the thermodynamic arguments leading to the hole-density being governed by the contact angle or wettability. From a simple model of thin film stability without considering any interfacial segregation or slip, the time scale for the appearance of holes is given by^{6,39}

$$\tau \sim (\mu/\gamma)[f(\theta)]^{-2} \quad (4)$$

where μ is the viscosity of the solvent-laden PS film and $f(\theta)$ is an increasing function of θ as announced before.

Further, the velocity, V , of hole growth (inverse of the time scale for hole growth)^{39,41–45} is given by

$$V \sim (\gamma/\mu)[F(\theta)] \quad (5)$$

where $F(\theta)$ is an increasing function of θ , which scales as θ^3 in the limit of very small contact angles (Tanner's law).

Both eqs 4 and 5 are physically sound in that they predict that the time scales of hole formation and growth should increase on a more wettable substrate (smaller contact angle) as the instability becomes weaker. However, the experimental kinetic results in Figures 4, 7 (velocity of contact line retraction in ethanol and *n*-hexane), and 8 (time scales for the appearance or formation of holes) show an opposite trend than the theory predictions related to the influence of contact angle! For example, addition of ethanol increases the contact angle and should thus decrease the time for the formation of holes and increase the contact-line velocity, but the observations are just the opposite. The case of *n*-hexane is even more striking, where a nonmonotonic larger variation of the contact angle is observed, but the experimental results on the kinetics are again counterintuitive to the theory in that one sees an increase in the time scales or a slowing down with an increase in the contact angle and vice versa. Clearly, the other factors that affect kinetics, such as the viscosity, interfacial tension, and the role of nonsolvent interfacial segregation,³³ need to be considered.

As argued before, interfacial segregation of ethanol at the substrate–film boundary is not likely because of a much lower affinity of ethanol for the silicon wafer as compared to acetone (Figure 9c). Thus, the major kinetic factor is the transport

limitation reflected in an increased viscosity aided maybe by a decrease in slippage, as discussed above. Both of these favor a reduction in the dewetting velocity. Adding of nonsolvents should decrease the mobility of PS chains owing to their increasing collapse with increased nonsolvent concentration. This factor could overwhelm the effect of changes brought about by a slight increase in the contact angle with an increased volume fraction of ethanol. A slowdown in the kinetics of holes formation and their subsequent growth also allows an opportunity for the growth of new holes in the areas which have not yet dewetted. This explains a greater propensity for a continued appearance of new holes with a nonsolvent (Figure 8) compared to acetone alone where all the holes appear rapidly in the initial phase and the hole-density remains nearly constant thereafter until the onset of coalescence. These scenarios of a near simultaneous or continuous formation of holes are also seen in the van der Waals destabilized thermally annealed films,^{12,39} but the influence of polar interactions in this process is not yet addressed.

Similarly, in the case of *n*-hexane as the nonsolvent, the variation of contact angle and the kinetics of hole growth are out-of-phase from theory. For example, the contact angle first decreases and then increase with the increase in the volume fraction of *n*-hexane, implying (without considering the change of the viscosity of the film) that the velocity of hole growth should first decrease and then increase. However, interestingly, the experimental results are opposite to this argument. In the first volume fraction regime (0–0.3), hole growth and hole formation become considerably faster, despite a substantial reduction in the contact angle and a putative increase in the viscosity owing to the presence of a nonsolvent! One should thus consider the interfacial segregation of hexane to play a profound role in this regime in greatly diminishing the friction and dissipation at the substrate, which is the rate-limiting factor determining the kinetics. As shown in Figure 9c, *n*-hexane indeed has a greater affinity for the substrate, as indicated by its complete spreading, which should allow slippage of the polymer chains. As discussed before, the decrease in the contact angle of the PS droplets in this regime also indicates the formation of an ultrathin *n*-hexane layer or enriched zone at the substrate surface. The presence of a low-viscosity interlayer replacing the high viscosity adhering polymer chains can greatly decrease the viscous friction and thus enhance the kinetics. With further increase in the volume fraction beyond 0.3, the effect of reduction in the interfacial friction reaches its limit, but the effect of increasing film viscosity with increased *n*-hexane content should now slow down the kinetics.

In order to get further insight into the possible modification of the substrate by *n*-hexane, we performed an additional experiment. In all of the experiments reported above, PS films were immersed directly in a preprepared acetone/*n*-hexane mixture. Now, a PS film was first placed in pure liquid *n*-hexane for a long time (90 min), allowing slow diffusion through the film but without any dewetting observed. Acetone was then rapidly added to hexane to form a mixture containing 5% volume fraction of hexane. The PS films dewetted in such a mixture, as expected. However, dewetting was faster in the film pre-equilibrated with hexane compared to the film that was directly placed in the mixture (Figure 10). This observation also indicates a greater modification of the substrate by *n*-hexane, which allows a faster kinetics once acetone is added.

We conclude by noting that the current understanding of thin polymer film dewetting is limited to pseudo-single-phase

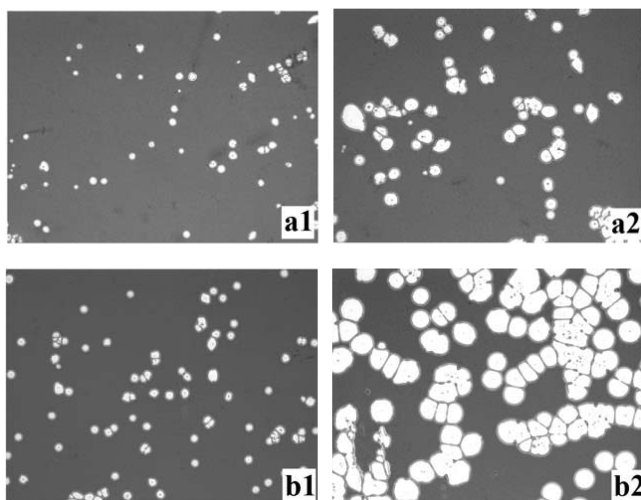


Figure 10. OM images of the morphology of PS films (67 ± 2 nm) placed either in a 5% *n*-hexane/acetone mixture (images a1 and a2) or pre-equilibrated in *n*-hexane for 90 min before addition of acetone to make a 5% *n*-hexane mixture (images b1 and b2). Morphologies in images a1 and b1 are at 20 s in the mixture and those of images a2 and b2 are at 60 s. The size of images are $300 \times 225 \mu\text{m}^2$.

films (melts) without considerations of very real polar interactions and interfacial segregation of liquid solvents/nonsolvents that may occur owing to their differing affinities to the substrate. The novel experimental results presented here point to the difficulties in reconciling the observations with simple theories without taking into account additional dimensions. In any case, it is clear that the spontaneous dewetting of a thin polymer film in mixed liquid solvents allows much greater control of the length and time scales compared to the widespread thermal and vapor phase annealing practices that exist.

CONCLUSIONS

We have investigated the equilibrium and dynamic aspects of spontaneous room-temperature dewetting of thin polymer films annealed under several liquid mixtures of a poor solvent (acetone) and a nonsolvent. Dewetting is characterized by the number density of holes (length scale) and the kinetics of hole formation and growth. The polystyrene films on the oxide stripped silicon wafers considered are stable in air and resistant to dewetting by thermal annealing. Their dewetting under the solvent mixture (acetone/ethanol or acetone/*n*-hexane) proceeds by the introduction of polar interactions. The nature of the nonsolvent, its affinity with the substrate vis-à-vis the solvent and its volume fraction all govern the polymer equilibrium wettability, hole density, and the kinetic aspects, which are often nonintuitive and theoretically not well understood. For example, addition of a 0.2 volume fraction of ethanol (nonsolvent) increases the hole density by a factor of 20 while simultaneously slowing the kinetic processes by several orders despite a very small change in the wettability. This finding offers a general route to miniaturization of thin film dewetting patterns. Nonmonotonic changes in the hole density and kinetics are witnessed with increased *n*-hexane content that are again out-of-phase with each other, the hole density being in-phase with the contact angle and the kinetics being out-of-phase with the contact angle variation. An explanation of these observations requires considering the factors beyond the

customary properties like the polymer chain mobility (viscosity), film interfacial tension, and wettability (contact angle). Comparison with the existing theoretical ideas is more in the spirit of pointing out the gaps to motivate further work in the control of polymer thin film equilibrium and dynamics by annealing under liquid mixtures. We suggest that the greater affinity of a component to the substrate plays an important role in the formation of an ultrathin nanophase separated zone at the substrate–polymer interface that modifies the contact angle and viscous friction and dissipation. Thus, unlike thermal or solvent-vapor-induced dewetting, room temperature dewetting under the liquid mixtures offers a far greater control of the dewetting kinetics, shape of final droplets (contact angle), and pattern dimensions, even in the stable films.

AUTHOR INFORMATION

Corresponding Authors

*A.S. e-mail: ashutos@iitk.ac.in.

*T.S. e-mail: tfshi@ciac.jl.cn.

Notes

The authors declare no competing financial interest.

ACKNOWLEDGMENTS

This work is supported by the World Class University Grant No. R32-2008-000-20082-0 of the National Research Foundation of Korea, the National Natural Science Foundation of China (No. 21234007), and the Department of Science and Technology, India.

REFERENCES

- (1) Yoneda, H.; Nishimura, Y.; Doi, Y.; Fukuda, M.; Kohno, M. Development of Microporous PE Films To Improve Lithium Ion Batteries. *Polym. J.* **2010**, *42*, 425–437.
- (2) Wang, X.; Yakovlev, S.; Beers, K. M.; Park, M. J.; Mullin, S. A.; Downing, K. H.; Balsara, N. N. On the Origin of Slow Changes in Ionic Conductivity of Model Block Copolymer Electrolyte Membranes in Contact with Humid Air. *Macromolecules* **2010**, *43*, 5306–5314.
- (3) Sandstrom, A.; Matyba, P.; Inganäs, O.; Edman, L. Separating Ion and Electron Transport: The Bilayer Light-Emitting Electrochemical Cell. *J. Am. Chem. Soc.* **2010**, *132*, 6646–6647.
- (4) Siegel, A. P.; Murcia, M. J.; Johnson, M.; Reif, M.; Jordan, R.; Ruhe, J.; Naumann, C. A. Compartmentalizing a Lipid Bilayer by Tuning Lateral Stress in a Physisorbed Polymer-Tethered Membrane. *Soft Matter* **2010**, *6*, 2723–2732.
- (5) Huang, J. H.; Li, K. C.; Kekuda, D.; Padhy, H. H.; Lin, H. C.; Ho, K. C.; Chu, C. W. Efficient Bilayer Polymer Solar Cells Possessing Planar Mixed-Heterojunction Structures. *J. Mater. Chem.* **2010**, *20*, 3295–3300.
- (6) Sharma, A. Relationship of Thin Film Stability and Morphology to Macroscopic Parameters of Wetting in the Apolar and Polar Systems. *Langmuir* **1993**, *9*, 861–869.
- (7) Bandyopadhyay, D.; Sharma, A. Self-Organized Microstructures in Thin Bilayers on Chemically Patterned Substrates. *J. Phys. Chem. C* **2010**, *114*, 2237–2247.
- (8) Lim, S. K.; Perrier, S.; Neto, C. Patterned Chemisorption of Proteins by Thin Polymer Film Dewetting. *Soft Matter* **2013**, *9*, 2598–2602.
- (9) Akhrass, S. A.; Reiter, G.; Hou, S. Y.; Yang, M. H.; Chang, Y. L.; Chang, F. C.; Wang, C. F.; Yang, A. C.-M. Viscoelastic Thin Polymer Films under Transient Residual Stresses: Two-Stage Dewetting on Soft Substrates. *Phys. Rev. Lett.* **2008**, *100*, 178301.
- (10) Besancon, B. M.; Green, P. F. Dewetting Dynamics in Miscible Polymer–Polymer Thin Film Mixtures. *J. Chem. Phys.* **2007**, *126*, 224903.

- (11) Karapanagiotis, I.; Gerberich, W. W. Polymer Film Rupturing in Comparison with Leveling and Dewetting. *Surf. Sci.* **2005**, *594*, 192–202.
- (12) Becker, J.; Grün, G.; Seemann, R.; Mantz, H.; Jacobs, K.; Mecke, K.; Blossey, A. Complex Dewetting Scenarios Captured by Thin-Film Models. *Nat. Mater.* **2003**, *2*, 59–63.
- (13) Reiter, G.; Khanna, R. Kinetics of Autophobic Dewetting of Polymer Films. *Langmuir* **2000**, *16*, 6351–6357.
- (14) Sharma, A.; Khanna, R. Pattern Formation in Unstable Liquid Films. *Phys. Rev. Lett.* **1998**, *81*, 3463–3466.
- (15) Reiter, G. Dewetting of Thin Polymer Films. *Phys. Rev. Lett.* **1992**, *68*, 75–78.
- (16) Reiter, G.; Akhrass, S. A.; Hamieh, M.; Damman, P.; Gabriele, S.; Vilmin, T.; Raphaël, E. Dewetting as an Investigative Tool for Studying Properties of Thin Polymer Films. *Eur. Phys. J. Spec. Top.* **2009**, *166*, 165–172.
- (17) Volodin, P.; Kondyurin, A. Dewetting of Thin Polymer Film on Rough Substrate: II. Experiment. *J. Phys. D: Appl. Phys.* **2008**, *41*, 065307.
- (18) Xu, L.; Sharma, A.; Joo, S. W. Instability and Pattern Formation Induced in Thin Crystalline Layers of a Conducting Polymer P3HT by Unstable Carrier Films of an Insulating Polymer. *J. Phys. Chem. C* **2012**, *116*, 21615–21621.
- (19) Xie, R.; Karim, A.; Douglas, J. F.; Han, C. C.; Weiss, R. A. Spinodal Dewetting of Thin Polymer Films. *Phys. Rev. Lett.* **1998**, *81*, 1251–1254.
- (20) Meredith, J. C.; Smith, A. P.; Karim, A.; Amis, E. J. Combinatorial Materials Science for Polymer Thin-Film Dewetting. *Macromolecules* **2000**, *33*, 9747–9756.
- (21) Gabriele, S.; Sclavons, S.; Reiter, G.; Damman, P. Disentanglement Time of Polymers Determines the Onset of Rim Instabilities in Dewetting. *Phys. Rev. Lett.* **2006**, *96*, 156105.
- (22) Gabriele, S.; Damman, P.; Sclavons, S.; Desprez, S.; Coppée, S.; Reiter, G.; Hamieh, M.; Akhrass, S. A.; Vilmin, T.; Raphaël, E. Viscoelastic Dewetting of Constrained Polymer Thin Films. *J. Polym. Sci., Polym. Phys.* **2006**, *44*, 3022–3030.
- (23) Yang, Z. H.; Fujii, Y.; Lee, F. K.; Lam, C.-H.; Tsui, O. K. C. Glass Transition Dynamics and Surface Layer Mobility in Unentangled Polystyrene Films. *Science* **2010**, *328*, 1676–1679.
- (24) Clough, A.; Peng, D. D.; Yang, Z. H.; Tsui, O. K. C. Glass Transition Temperature of Polymer Films That Slip. *Macromolecules* **2011**, *44*, 1649–1653.
- (25) Yang, Z. H.; Clough, A.; Lam, C.-H.; Tsui, O. K. C. Glass Transition Dynamics and Surface Mobility of Entangled Polystyrene Films at Equilibrium. *Macromolecules* **2011**, *44*, 8294–8300.
- (26) Lee, S. H.; Yoo, P. J.; Kwon, S. J.; Lee, H. H. Solvent-Driven Dewetting and Rim Instability. *J. Chem. Phys.* **2004**, *121*, 4346–4351.
- (27) Xu, L.; Shi, T. F.; An, L. J. The Dewetting Dynamics of The Polymer Thin Film by Solvent Annealing. *J. Chem. Phys.* **2008**, *129*, 044904.
- (28) Fondecave, R.; Brochard-Wyart, F. Polymers as Dewetting Agents. *Macromolecules* **1998**, *31*, 9305–9315.
- (29) Kim, H. I.; Mate, C. M.; Hannibal, K. A.; Perry, S. S. How Disjoining Pressure Drives The Dewetting of a Polymer Film on a Silicon Surface. *Phys. Rev. Lett.* **1999**, *82*, 3496–3499.
- (30) Bormashenko, E.; Pogreb, R.; Musin, A.; Stanevsky, O.; Bormashenko, Y.; Whyman, G.; Barkay, Z. Patterning in Rapidly Evaporated Polymer Solutions: Formation of Annular Structures under Evaporation of the Poor Solvent. *J. Colloid Interface Sci.* **2006**, *300*, 293–297.
- (31) Verma, A.; Sharma, A. Enhanced Self-Organized Dewetting of Ultrathin Polymer Films under Water–Organic Solutions: Fabrication of Sub-Micrometer Spherical Lens Arrays. *Adv. Mater.* **2010**, *22*, 5306–5309.
- (32) Verma, A.; Sharma, A. Sub-40 nm Polymer Dot Arrays by Self-Organized Dewetting of Electron Beam Treated Ultrathin Polymer Films. *RSC Adv.* **2012**, *2*, 2247–2249.
- (33) Xu, L.; Sharma, A.; Joo, S. W. Dewetting of Stable Thin Polymer Films Induced by a Poor Solvent: Role of Polar Interactions. *Macromolecules* **2012**, *45*, 6628–6633.
- (34) Siretanu, I.; Chapel, J. P.; Drummond, C. Water–Ions Induced Nanostructuring of Hydrophobic Polymer Surfaces. *ACS Nano* **2011**, *5*, 2939–2947.
- (35) Siretanu, I.; Chapel, J. P.; Drummond, C. Substrate Remote Control of Polymer Film Surface Mobility. *Macromolecules* **2012**, *45*, 1001–1005.
- (36) Rubinstein, M.; Colby, R. H. *Polymer Physics*; Oxford University Press: Oxford, UK, 2003; pp 144, 174.
- (37) Reiter, G. Unstable Thin Polymer Films: Rupture and Dewetting Processes. *Langmuir* **1993**, *9*, 1344–1351.
- (38) Reiter, G.; Khanna, R.; Sharma, A. Enhanced Instability in Thin Liquid Films by Improved Compatibility. *Phys. Rev. Lett.* **2000**, *85*, 1432–1435.
- (39) Sharma, A. Many Paths to Dewetting of Thin Films: Anatomy and Physiology of Surface Instability. *Eur. Phys. J. E* **2003**, *12*, 397–408.
- (40) Kajari, K.; Sharma, A.; Khanna, R. Instability, Dynamics, and Morphology of Thin Slipping Films. *Langmuir* **2004**, *20*, 244–253.
- (41) Brochard-Wyart, F.; de Gennes, P. G.; Hervet, H.; Redon, C. Wetting and Slippage of Polymer Melts on Semi-Ideal Surfaces. *Langmuir* **1994**, *10*, 1566–1572.
- (42) Brochard-Wyart, F.; Debrégeas, G.; Fondecave, R.; Martin, P. Dewetting of Supported Viscoelastic Polymer Films: Birth of Rims. *Macromolecules* **1997**, *30*, 1211–1213.
- (43) Brochard-Wyart, F.; Daillant, J. Drying of Solids Wetted by Thin Liquid Films. *Can. J. Phys.* **1990**, *68*, 1084–1088.
- (44) Jacobs, K.; Seemann, R.; Schatz, G.; Herminghaus, S. Growth of Holes in Liquid Films with Partial Slippage. *Langmuir* **1998**, *14*, 4961–4963.
- (45) Seemann, R.; Herminghaus, S.; Neto, C.; Schlagowski, S.; Podzimek, D.; Konrad, R.; Hubert Mantz, H.; Jacobs, K. Dynamics and Structure Formation in Thin Polymer Melt Films. *J. Phys.: Condens. Matter* **2005**, *17*, S267–S290.
- (46) Seemann, R.; Herminghaus, S.; Jacobs, K. Dewetting Patterns and Molecular Forces: A Reconciliation. *Phys. Rev. Lett.* **2001**, *86*, 5534–5537.
- (47) Sherrington, D. C. Preparation, Structure and Morphology of Polymer Supports. *Chem. Commun.* **1998**, *21*, 2275–2286.
- (48) Sadek, P. *The HPLC Solvent Guide*; Wiley-Interscience Press: New York, 2002; p 23.